1st IMEKO TC-4 International Workshop on
Metrology for Geotechnics
Benevento, Italy, March 17-18, 2016

Compression and extension triaxial tests on sand, studied with X-ray microtomography and digital image correlation

Salvatore E.[1], Andò E.[2], Viggiani G.[2], Modoni G.[1]

[1] *University of Cassino and Southern Lazio, via G. di Biasio 43, 03043 Cassino, e.salvatore@unicas.it, modoni@unicas.it*

[2] *Grenoble-INP/UJF-Grenoble 1/CNRS UMR 5521, Laboratoire3SR, Grenoble, France edward.ando@3sr-grenoble.fr; cino.viggiani@3sr-grenoble.fr*

***Abstract* – In the usual execution of triaxial tests, the longitudinal and volumetric strains are computed cumulatively from displacements measured outside the sample, and thus interpretation is based on the implicit assumption that samples deform homogeneously. This evident misconception often leads to inconsistent sometimes surprising results, mostly near failure where intensive strain localization usually takes place. Aiming to observe the distribution of strains, a series of triaxial compression and extension tests have been carried out at the Laboratoire 3SR of Grenoble. The tests have been performed on small samples of a uniform sand, tracking the particles movement with x-ray tomography and digital image correlation. This paper illustrates this experimental technique and the methodology adopted for image processing with reference to selected experimental results. The results show that strains tend to concentrate in smaller portions of the sample, starting from early loading steps and evolve in largely different ways for compression and extension tests depending on the applied confining stress.**

I INTRODUCTION

In the ordinary practice, the study of the mechanical behaviour of geomaterials is approached by adopting the simplified scheme of continuum, purposely neglecting the particulate nature of the material. In fact, the applied forces are assumed to distribute homogeneously within the sample and displacement are measured at the specimen's boundaries by considering a homogeneous deformation of the sample.

However, it is common experience that both natural and man-made soil structure often show a heterogeneous state of deformation, eventually ending up in failure surfaces concentrated within narrow zones. This phenomenon, known as strain localization, is commonly encountered in laboratory tests and has been experimentally and theoretically studied since the 1970's [1, 2, 3].

The paper aims to experimentally investigate the role of the strain localization phenomenon on the macroscopic phenomenological approach commonly adopted in mechanical tests, by means a set of triaxial extension tests carried out on Hostun sand (H31) inside the X-ray scanner housed in the 3SR laboratories of Grenoble. The reconstructed three dimensional images of the specimens during the shear process, combined with Digital Image Correlation and digital porosity computing, allowed to quantitatively investigate the different mechanisms of deformation taking place in the material. The obtained results are compared with triaxial compression tests on the same material and confining pressures coming from [4].

II EXPERIMENTAL CAMPAIGN

A. *Material studied*

The experimental campaign has been carried out on Hostun sand H31, extensively used in 3SR Laboratory as reference material. It has a colour that ranges between grey-white and rosy-beige, while its chemical components consist in high siliceous amount (SiO_2 >98%).

In particular, the H31 sand is characterized by a specific gravity G_S=2.65, main particle diameter D_{50} of 0.35mm and coefficient of uniformity C_u equal to 1.7 (Figure 1). The SEM pictures in Figure 2, reveal that grain shape varies from angular to sub-angular.

B. *Experimental program*

The experiments analysed in this paper are two triaxial extension tests performed at 100kPa and 3Mpa confining stress (Table 1), both performed on dry material.

Following the methodology proposed in [4], small specimens, having 11mm diameter and 22mm height,

ISBN: 978-92-990075-0-1

have been prepared by pluviating the material into a membrane stretched against a mould through a 1m height plastic tube with a funnel on the top.

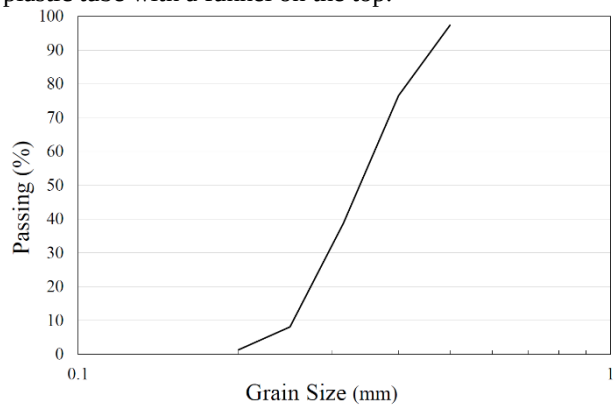

Figure 1 Grain size distribution of Hostun sand H31 (from the manufacturer, [5]).

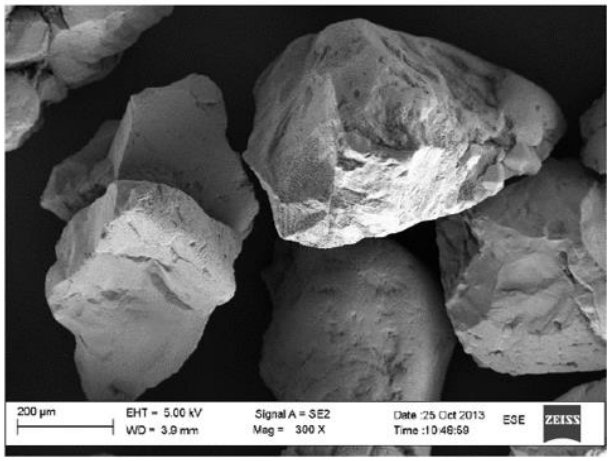

Figure 2 Scanning Electron Microscope of Hostun sand H31.

Table 1 Experimental program.

ID test	Strain path	Confining pressure (kPa)	e_0
HNEES02	Extension	100	0.70
HHEES02	Extension	3000	0.68

In order to ensure a constant drop height of the material, the pluviation system is lifted with about the same rate as the advance of the top of the specimen.

Once the specimen is prepared, 30kPa of vacuum is applied to install it into the triaxial cell. Here the sample is isotropically consolidated up to the desired stress level by increasing the pressure of the confinement fluid and simultaneously releasing the inner vacuum.

In order to perform X-ray tomography of the specimen without any disturbance, the cell is made of polycarbonate without any steel tie-bar. Depending on the confining pressure, different cell fluids and membranes are adopted: water with 300µm thick latex membrane for low confinement pressure tests, oil and 500µm thick neoprene membranes for high pressure tests.

Once the isotropic phase is completed, the sample has been left rest for 30 minutes to complete the majority of the viscous strains; therefore, the shear phase has been performed by pulling the sample at the strain controlled rate of 21µm/min.

During the test, loading is temporarily interrupted to perform scanning while axial displacement is kept constant. In the scanning time, some relaxation of the axial stress is noticed starting immediately after loading interruption.

Every scan is performed with X-ray radiograph while the sample is rotated around its vertical axis. By a fine adjustment of the distance between photons' source and sample (Figure 3), a pixel size of 20µm may be scanned, thus giving a good representation at the grain scale. Finally, a digital image, 1250x1250x1600pixel, describing the 3D X-ray linear attenuation field of the specimen is obtained for each loading step, by rebuilding the whole set of the acquired radiographs.

For each pair of subsequent reconstructed digital images of the specimen DIC is applied by running the code Tomowarp2 developed in Laboratoire 3SR.

Digital Image Correlation is a mathematical tool matching one digital image with another. Firstly, a three-dimensional grid of nodes is defined in the two images and a correlation window is created around each of them; therefore, for each node of the reference image, the corresponding window in the target one is moved pixel by pixel in the three directions into a search space and a correlation coefficient quantifying the resemblance between the extracted three-dimensional patterns is computed. The process ends up providing the displacement of the node (u_x, u_y, u_z, φ_x, φ_y, φ_z) as the displacement of the correlation window corresponding to the higher correlation coefficient. Once the displacement of each node is measured with subpixel precision, the 3D strain tensor is computed.

Porosity distribution for granular materials is of paramount importance, especially in the light of the results concerning the strain localization phenomenon. In the present study, the porosity map of the sample is obtained by working on the reconstructed images (in grey-scale) by using a software deployed in 3SR. The software, for each node on a regularly spaced grid defines a subvolume (1500x1500x1500µm) in which any voxel having a grey-scale value equal to, or higher than, the grain grey-scale is identified in 100% solid, and any voxel having a grey-scale value equal to, or lower than, the pore grey-scale value in 100% pore, while the grey-scale values between these two limits are linearly interpolated. The two threshold values are measured manually on a small selection of pores and grains in the sample.

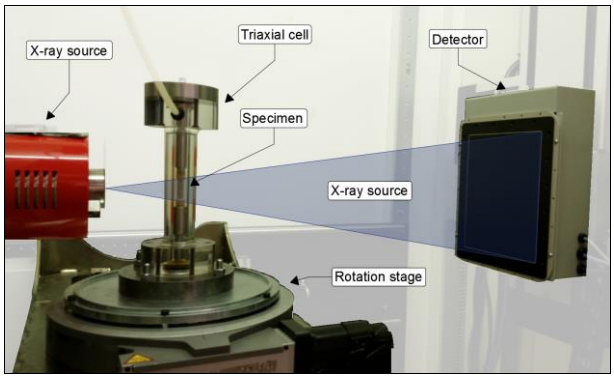

Figure 3 Setup of the testing apparatus.

III EXPERIMENTAL RESULTS

A. Macroscopic results

In Figure 4 the results of two triaxial extension tests are represented in terms of deviatoric stress and volumetric strain plotted versus axial strain. In this plot deformation are macroscopically computed. In the same figure, results of triaxial compression tests on the same material and confining stresses are plotted [4] (Table 2).

Table 2 Main characteristics of tests coming from [4].

ID test	Strain path	Confining pressure (kPa)	e_0
HNEA01	Compression	100	0.61
HHEA06	Compression	3000	0.52

For both the strain paths, in accordance with previous studies concerning granular materials [6, 7], the increase of confining pressure produces an increase of resistance and stiffness, with a transition from fragile-dilatant to ductile-contractive behaviour.

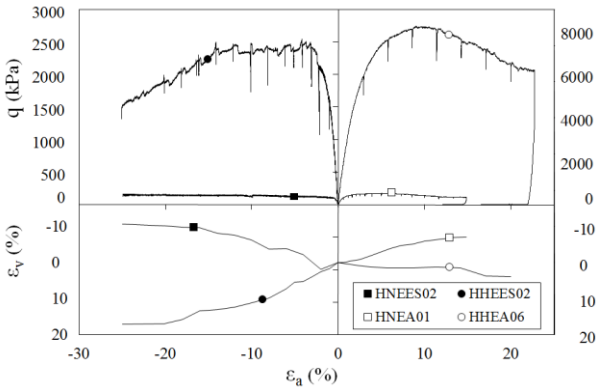

Figure 4 Results of the triaxial extension tests HNEES02 and HHEES02 compared with triaxial compression tests at the same confinement pressures [4].

B. Microscopic image analysis

In Table 3 several vertical slices are plotted reporting the increment of the second invariant of the strain tensor and the porosity fields for the most significant loading step of the performed tests.

In the test performed at lower confining pressure (HNEES02), the evolution of shear field evolution reveals that homogeneity is lost from very low strain values. In particular, the maximum shear field is characterized by three butterfly shaped patterns localized in the middle and at the ends of the specimen. This test shows that, despite the exterior appearance of the specimens gives the feeling of a homogeneous deformation, the true strain field is localized. A similar observation was presented in [3] by carrying out a triaxial compression test on the same material at 60kPa confining pressure. Using X-ray tomography, the author showed that the apparent homogenous barrel shape commonly assumed by compressed specimens was just the external result of a complicate pattern of strain localization.

The porosity field analysis confirms the heterogeneity of the strain field even from the volumetric viewpoint. In fact, the images show an increasingly dilatant behaviour of the material as the specimen is sheared. Apart from the volume where the shear strain localization takes place, the volume in the remaining portion of the sample remains almost constant.

In the test carried out at higher confining pressure (HHEES02), the image correlation shows a strong dynamic evolution of the strain localization pattern. After the first stretching step (ε_a=0÷-1%) in which the specimen undergoes a quite uniform deformation, the strain localization appears in the upper part of the specimen and progressively translates downward, before heading to a strong reduction of the cross section (necking). Contemporarily, the material moves from a condition where shear strains are quite uniformly distributed along the height of the specimen (ε_a=-4÷-5%). As for the lower confinement test, the porosity field evolves in a not uniform distribution leading to higher porosity in correspondence of the necked zone.

To reach a deeper understanding on the deformation mechanisms taking place in sheared sand, the above results obtained with extension tests, are compared with the results shown in Table 4 coming from [4]. Again, the maximum shear and porosity fields evolution described in Table 4, show a highly localized pattern of strains ending up in narrow shear bands. The sample undergoes deformation just in this zone, while the outer part remains almost inactive. This tendency is confirmed by several previous works by using different investigation techniques as pulse wave transmission tests [8, 9, 10].

In Table 5 the inclination of the shear bands respect to the maximum principal stress direction are reported for the tests studied in this work. The collected data show less pronounced inclination of the localization surfaces in triaxial extension then in compression.

Table 3 Maximum shear and porosity fields for the performed tests HNEES02 and HHEES02.

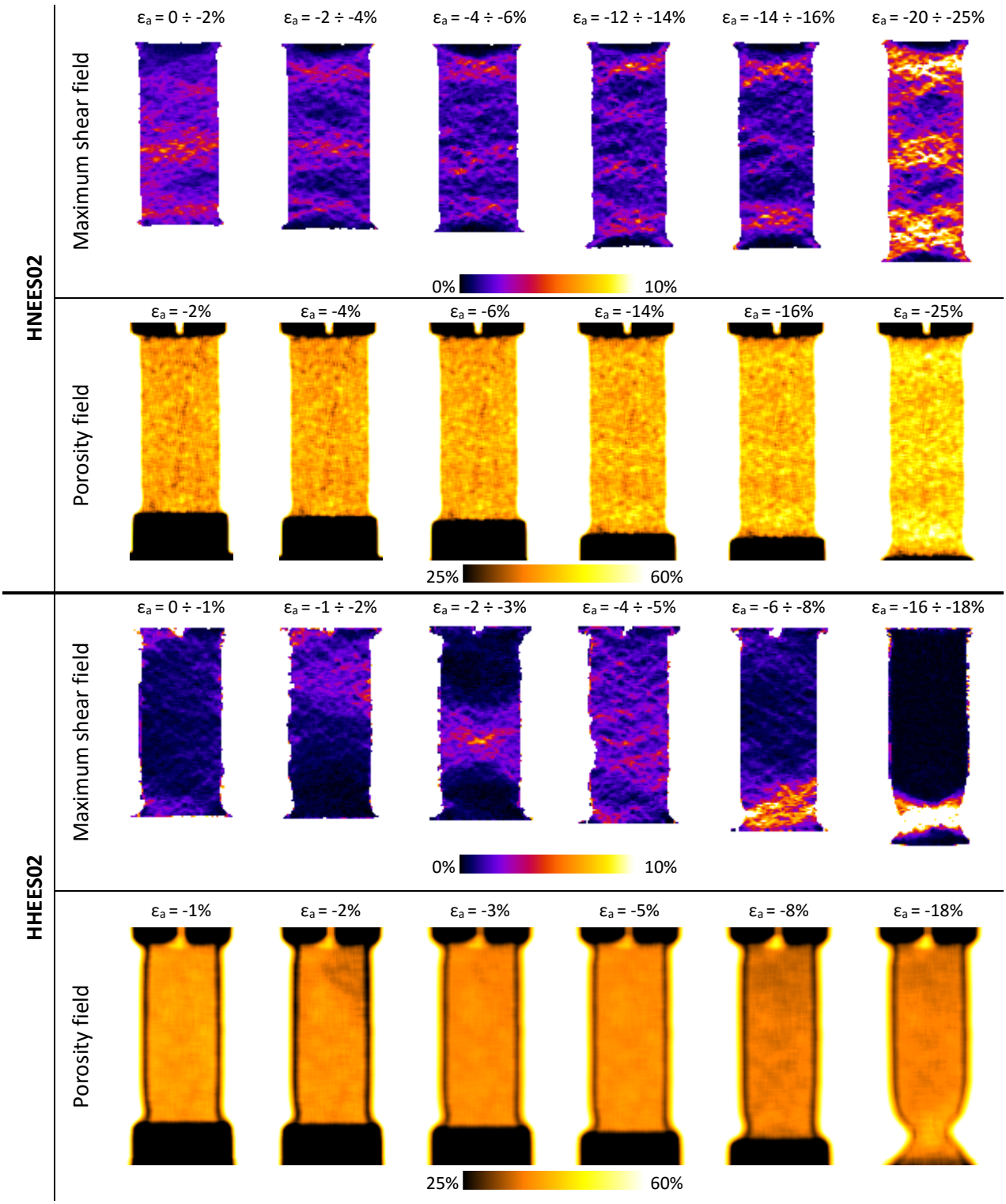

Table 4 Maximum shear and porosity fields for tests HNEA01 and HHEA06, [4].

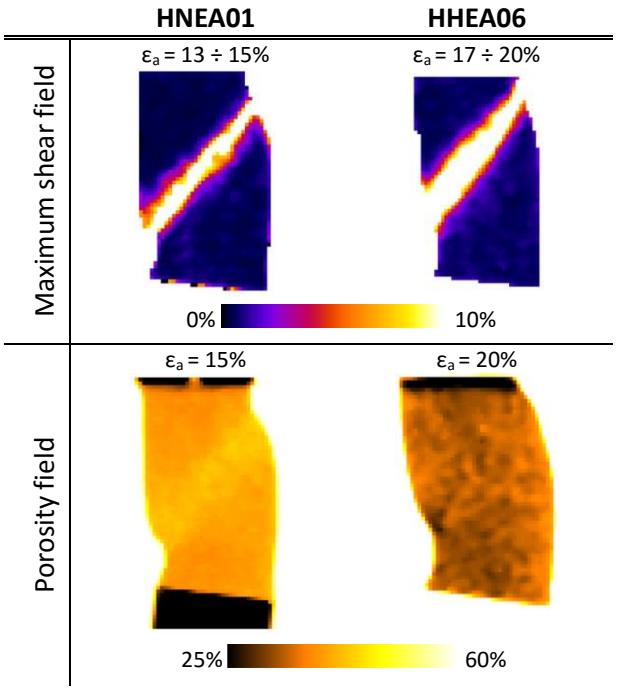

Table 5 Shear bands inclination respect to the maximum principal stress direction.

HNEES02	HHEES02	HNEA01	HHEA06
32.1°	31.5°	39.8°	38.1°

IV CONCLUSIONS

This study highlights the tendency of sands subjected to triaxial tests to concentrate deformation in relatively narrow zones. This result occurs both on compressed or extended samples.

At the highest axial strain, e.g. when steady state takes place [11], there is a meaningful difference between compression and extension test, both in terms of second invariant of the strain tensor or in porosity. The differences among the sample can reach one order of magnitude. In this situation, important doubts arise on the meaning of critical state.

Higher confining pressures seems to emphasize the strain localization phenomena by inducing necking; an explanation might be found in the weaker frictional forces developed at the lower confining pressure between soil and confining plates.

REFERENCES

[1] Rudnicki, J. W., and Rice J. R., (1975), Conditions for the localization of deformation in pressure-sensitive dilatant materials, Journal of the Mechanics and Physics of Solids 23 (6), 371-394.

[2] Vardoulakis, I., Goldscheider M, and Gudehus G., (1978). Formation of shear bands in sand bodies as a bifurcation problem, International Journal for numerical and analytical methods in Geomechanics 2 (2): 99-128.

[3] Desrues, Jacques, (2004). Tracking strain localization in geomaterials using computerized tomography, X-ray CT for Geomaterials, 15-41.

[4] Alikarami R., Andò E., Gkiousas Kapnisis M., Torabi A., Viggiani G., (2015). Strain localisation and grain breakage in sand under shearing at high mean stress: insights from in situ X-ray tomography, Acta Geotechnica 10 (1), 15-30.

[5] Sibelco France. Fiche Technique Type HN31, 2011 http://www.sibelco.fr/item_img/medias/images/ft12_hn31.pdf

[6] Modoni, G., Koseki J., and Anh Dan L.Q, (2010). Cyclic stress–strain response of compacted gravel. Géotechnique 61 (6), 473-485.

[7] Balakrishnaiyer, K., Koseki, J., Modoni, G., AnhDan, L. Q., Tatsuoka, F. (1998). Deformation characteristics at small strain levels of dense gravel. Geotechnics of Hard Soils and Soft Rocks, eds. by Evangelista and Picarelli, Balkema, 1, 423-430.

[8] Modoni G., Flora A., Mancuso C., Tatsuoka F., Viggiani C., (2000). Evaluation of gravel stiffness by pulse wave transmission tests. Geotechnical Testing Journal, 23 (4),506-521, ASTM.

[9] Flora, A., & Lirer, S. (2013). Small strain shear modulus of undisturbed gravelly soils during undrained cyclic triaxial tests. Geotechnical and Geological Engineering, 31(4), 1107-1122.

[10] Flora, A., Lirer, S., & Silvestri, F. (2012). Undrained cyclic resistance of undisturbed gravelly soils. Soil Dynamics and Earthquake Engineering, 43, 366-379.

[11] Schofield, A., Wroth P., (1968). Critical state soil mechanics. McGraw-Hill Book Co., London, p. 310.